[redacted]

RESEARCH MEMORANDUM

THE EFFECT ON ZERO-LIFT DRAG OF AN INDENTED FUSELAGE OR A THICKENED WING-ROOT MODIFICATION TO A 45° SWEPTBACK WING-BODY CONFIGURATION AS DETERMINED BY FLIGHT TESTS AT TRANSONIC SPEEDS

By William B. Pepper

Langley Aeronautical Laboratory
Langley Field, Va.

NATIONAL ADVISORY COMMITTEE FOR AERONAUTICS

WASHINGTON
September 20, 1951

[redacted]

Classification cancelled (or changed to Unclassified

By Authority NASA Tech Pub Announcement

94 11 Jan 56

By

GRADE OF OFFICER MAKING CHANGE)

16 Jan 61

DATE

NATIONAL ADVISORY COMMITTEE FOR AERONAUTICS

RESEARCH MEMORANDUM

THE EFFECT ON ZERO-LIFT DRAG OF AN INDENTED FUSELAGE OR A THICKENED WING-ROOT MODIFICATION TO A 45° SWEPTBACK WING-BODY CONFIGURATION AS DETERMINED BY FLIGHT TESTS AT TRANSONIC SPEEDS

By William B. Pepper

SUMMARY

Rocket-powered models were flown at transonic speeds to determine the effect on the zero-lift drag coefficient of an indented fuselage modification and of a thickened wing-root modification of a swept-wing airplane configuration. The unmodified wing-body that was used for comparison consisted of a wing swept back 45° along the quarter-chord line, aspect ratio 6.0, taper ratio of 0.6, and NACA 65A009 airfoil section in the free-stream direction and a fuselage of fineness ratio 10.0. The modified-fuselage configuration had a two-dimensional indentation perpendicular to the wing plane starting at the intersection of the wing leading edge and the fuselage. The modified-wing configuration had a wing that increased in thickness linearly from 9 percent at 40 percent of the semispan to 16 percent at the fuselage center line.

The total drag coefficient of the unmodified model was 0.015 at a Mach number of 0.9, 0.038 at a Mach number of 1.10, and 0.044 at a Mach number of 1.25. Neither the thickened wing root nor the indented fuselage affected the subsonic drag of the configuration from a Mach number of 0.8 to 0.9. The thickened wing-root modification lowered the drag-rise Mach number of the configuration approximately 0.03 and caused an increase in the total drag coefficient varying from 5 percent at a Mach number of 1.10 to 3 percent at a Mach number of 1.25. The modified fuselage did not alter the drag-rise Mach number of the configuration but resulted in a decrease of the total drag coefficient varying from 12 percent at a Mach number of 1.10 to 5 percent at a Mach number of 1.25.

[redacted]

INTRODUCTION

As part of a general transonic research program of the National Advisory Committee for Aeronautics to determine the aerodynamic properties of promising configurations, rocket-propelled models were tested in free flight to determine the effect on zero-lift drag of two exploratory wing-body-juncture modifications of a transonic airplane configuration. Some wing-plus-interference drag coefficients were also determined.

Much theoretical and experimental work has been directed toward the modification of the fuselage shape in the vicinity of the wing root in an attempt to delay the drag-rise Mach number of the configuration (references 1 and 2). This type of fuselage modification, however, has not been investigated at transonic or supersonic speeds. The present investigation is designed to explore the possibilities of reducing wing-body interference throughout the transonic region.

At present, the most effective method of delaying the drag rise and reducing the transonic wing-body drag is to use thin sweptback wings. The structural problems of designing and building very thin swept wings to withstand the loads encountered in transonic flight, however, are considerable. A possible recourse would be a wing with thin outboard sections and thicker root sections. The structural benefits gained by a thickened wing root must be balanced against the possible adverse effects on the drag coefficient. Experimental results in reference 3 for nacelles mounted near the wing root showed favorable low drag which led to the hope that thickness could be added near the wing root without undue penalty. The modified wing root was designed to explore this possibility.

Drag coefficients of the configurations tested are presented over a continuous Mach number range of 0.8 to 1.25. The corresponding Reynolds number range was from 3.3×10^6 to 7.1×10^6 when it was based on the mean aerodynamic chord of the wing.

SYMBOLS

b	wing span
C_{D_T}	total drag coefficient, based on S_W
C_{D_W}	wing-plus-interference drag coefficient, based on S_W
M	Mach number

R Reynolds number, based on wing mean aerodynamic chord of 0.822 feet

S_W total wing plan-form area (including part in fuselage), 3.878 square feet

r fuselage radius, inches

x wing or body station, inches

y wing ordinate, inches

z fuselage modification ordinate, inches

MODELS

The basic wing-body-fin configuration is the same as was used in references 3 and 4 and is shown in figure 1. The wing and fuselage coordinates are shown in tables 1 and 2. This model consisted of a fuselage of fineness ratio 10 with a sweptback wing mounted so that the leading edge intersected the fuselage at its maximum diameter. The wing had a sweepback of 45° along the quarter-chord line, an NACA 65A009 airfoil section in the free-stream direction, a taper ratio of 0.6, and an aspect ratio of 6.0 based on the total wing area of 3.878 square feet. Two fuselage models like that shown in figure 2 were tested. These two models had four stabilizing fins identical to the two fins on the winged model shown in figure 1.

The modified fuselage model shown in figure 3(a) has a two-dimensional indentation made up of straight-line elements perpendicular to the wing plane and starting at the intersection of the wing leading edge and the body. The ordinates for the fuselage modification are shown in table 1 and photographs of the model are shown in figure 4. The fuselage indentation was designed to approximate the streamline flow over an infinite wing of the same thickness and sweep by the following procedure:

1. Select a free-stream design Mach number of $M_o = 1.03$ with a free-stream velocity $V_o = 800$ feet per second.

2. Resolve V_o into a component V_n perpendicular to the wing maximum thickness line and a component V_p parallel to the maximum thickness line.

3. Obtain the ratio of local velocity v to undisturbed velocity V_n for incompressible flow over an airfoil section perpendicular to the maximum thickness line. (See reference 5.)

4. Use the value of V_n corresponding to the assumed value of M_o and solve for v over the airfoil.

5. Obtain the resultant velocity and direction by combining V_p and v.

6. Determine the streamline by progressively laying out the slope of the resultant velocity vectors starting from the intersection of the wing leading edge and the fuselage. The sharp discontinuity of the resultant streamline at the leading edge of the wing was eliminated by fairing in the streamline tangent to the fuselage. The minimum value of the derived Z coordinate occurred at a point 49 inches from the fuselage nose. The derived Z coordinate tended to increase in magnitude rearward of the minimum but this increase was replaced by a straight section parallel to the fuselage center line and a smooth fairing between the straight section and the fuselage. (See table 1.) The sharp intersection between the straight-line elements of the identation and the original fuselage surface was faired with a constant 1-inch radius.

The modified wing model is shown in figure 3(b) and a photograph of the model is presented in figure 5. The model tested had a wing which varied in thickness linearly from 9 percent at 40 percent of the semispan to 16 percent at the fuselage center line.

TESTS AND MEASUREMENTS

Four rocket-propelled zero-lift models were tested at the Langley Pilotless Aircraft Research Station at Wallops Island, Va. For convenience the models will be referred to as follows:

Model	Description
A, B	Unmodified fuselage, four fins
C	Unmodified fuselage, unmodified wing, two fins (reference 4)
D	Modified fuselage, unmodified wing, two fins
E	Unmodified fuselage, modified wing, two fins

Each model was propelled by a two-stage rocket system and launched from a rail launcher (fig. 6). The first stage or booster consisted of a 5-inch, lightweight, HVAR aircraft rocket motor (having a thrust of 5500 pounds for 0.95 second) that served to accelerate the model from zero velocity to high subsonic speeds. After the drag separation of the booster, a 3.25-inch Mk 7 aircraft rocket motor (delivering 1730 pounds thrust for 1.0 second) which was installed in the model accelerated it to supersonic speeds. Tracking instrumentation consisting of a CW Doppler radar set and an NACA modified SCR 584 radar tracking unit was used to determine the flight path and deceleration during the coasting flight. A survey of atmospheric conditions at the time of each launching was made through radiosonde measurements from an ascending balloon.

The values of drag coefficient were calculated as in reference 6. The order of accuracy of the total drag coefficient as determined in reference 4 is ±0.0004. The Mach number was determined from the velocity of each model and the speed of sound at altitude from corresponding radiosonde records. The accuracy of the Mach number determination is estimated to be within ±0.005.

RESULTS AND DISCUSSION

Flight tests of the models covered a Reynolds number range from 3.3×10^6 at $M = 0.8$ to 7.1×10^6 at $M = 1.25$ as shown in figure 7.

The variation of drag coefficient with Mach number for the two body-fin models (A and B) is presented in figure 8. The drag of two fins has been estimated by taking half of the difference in drag of two experimental research models with the same body as was used in reference 6, one with four fins at the base and one with no fins. These fins were identical to those of the present tests. Subtracting the drag coefficient of two fins from the average curve of models A and B gives an estimated curve for the fuselage with two fins which may be used to determine wing-plus-interference drag.

The variations in total drag coefficient with Mach number of the complete models are presented in figure 9(a). The effect of the wing and fuselage modifications on the total drag coefficient of the configuration is shown by comparison of the modified models D and E with the unmodified model C. The curve for model C is the average of three identical models presented in reference 4. The drag coefficient of the unmodified configuration varied from 0.038 at a Mach number of 1.10 to 0.0440 at $M = 1.25$ with a subsonic level of 0.015 at $M = 0.9$.

The drag coefficient of the modified fuselage configuration (model D) showed no significant change from that of the unmodified model between a Mach number of 0.8 to 0.96. This result is similar to that of reference 2. Within the accuracy of the measurements the drag-rise Mach number was not changed by the modification. Above a Mach number of 0.97, the fuselage indentation caused a significant reduction in total drag coefficient varying from 12 percent of the unmodified configuration drag at a Mach number of 1.10 to 5 percent at $M = 1.25$.

As shown in figure 9(a), thickening the wing root did not alter the drag from a Mach number 0.8 to 0.9; however, the drag-rise Mach number of this configuration was reduced approximately 0.03. The drag coefficient of the thickened wing-root model was higher than the unmodified model above a Mach number of 0.9 and varied from 5 percent at $M = 1.10$ to 3 percent at $M = 1.25$.

Figure 9(b) shows the wing-plus-interference drag coefficients for the three models obtained by subtracting the estimated drag of the fuselage with two fins shown in figure 8 from the total drag coefficients of the models presented in figure 9(a). It is logically considered for this comparison that any change in body drag due to the indentation is part of the wing-plus-interference drag since the indentation would not be used if there were no wing. The accuracy of the absolute level of the wing-plus-interference drag coefficients is dependent upon the estimation of body and two-fin drag and is believed to be within ±0.001. The wing-plus-interference drag coefficient of the unmodified wing was 0.022 at $M = 1.10$ and 0.029 at $M = 1.25$. Drag data for a similar wing tested without a fuselage in the Langley high-speed 7- by 10-foot tunnel are also shown in figure 9(b). The two curves are seen to have similar shapes but are on different drag levels. There is probably favorable interference effects of the rocket model wing in the presence of the fuselage due to its rearward location on the fuselage as was found in reference 7. Some of this difference may be due to the lower Reynolds number of the Langley 7- by 10-foot-tunnel tests which was 1.5×10^6 compared to 5.0×10^6 for the present tests and to the basic differences of test technique as discussed in reference 8.

CONCLUSIONS

The drag of three different rocket-propelled free-flight wing and body configurations at zero lift has been measured. The unmodified configuration consisted of a 9-percent-thick wing swept back 45° mounted on a body of fineness ratio 10. Two modified models were tested; one with an indented fuselage and one with a thickened wing root. The unmodified configuration previously tested had a total drag coefficient of 0.015 at a Mach number of 0.9, 0.038 at a Mach number of 1.10, and 0.044 at a Mach number of 1.25. When these values are used, the following conclusions may be made:

1. Neither the thickened wing root nor the indented fuselage modification affected the subsonic drag coefficient from a Mach number of 0.8 to 0.9.

2. The indented fuselage modification caused a significant reduction in total drag coefficient above a Mach number of 0.97 varying from 12 percent at a Mach number of 1.10 to 5 percent at a Mach number of 1.25. This modification did not alter the drag-rise Mach number.

3. The thickened wing-root modification lowered the drag rise Mach number of the configuration by approximately 0.03. The total drag coefficient was increased above a Mach number of 0.9 and varied from 5 percent at a Mach number of 1.10 to 3 percent at a Mach number of 1.25.

Langley Aeronautical Laboratory
National Advisory Committee for Aeronautics
Langley Field, Va.

REFERENCES

1. Küchemann, D.: Design of Wing Junction, Fuselage, and Nacelles to Obtain the Full Benefit of Sweptback Wings at High Mach Number. Rep. No. Aero. 2219, British R.A.E., Aug. 1947.

2. Boddy, Lee E.: Investigation at High Subsonic Speeds of Methods of Alleviating the Adverse Interference at the Root of a Swept-Back Wing. NACA RM A50E26, 1950.

3. Pepper, William B., Jr., and Hoffman, Sherwood: Comparison of Zero-Lift Drags Determined by Flight Tests at Transonic Speeds of Symmetrically Mounted Nacelles in Various Spanwise Positions on a 45° Sweptback Wing and Body Combination. NACA RM L51D06, 1951.

4. Pepper, William B., Jr., and Hoffman, Sherwood: Transonic Flight Tests to Compare the Zero-Lift Drag of Underslung and Symmetrical Nacelles Varied Chordwise at 40 Percent Semispan of a 45° Sweptback, Tapered Wing. NACA RM L50G17a, 1950.

5. Loftin, Laurence K., Jr.: Theoretical and Experimental Data for a Number of NACA 6A-Series Airfoil Sections. NACA Rep. 903, 1948. (Formerly NACA TN 1368.)

6. Welsh, Clement J.: Results of Flight Tests to Determine the Zero-Lift Drag Characteristics of a 60° Delta Wing with NACA 65-006 Airfoil Section and Various Double-Wedge Sections at Mach Numbers from 0.7 to 1.6. NACA RM L50F01, 1950.

7. Mathews, Charles W., and Thompson, Jim Rogers: Comparison of the Transonic Drag Characteristics of Two Wing-Body Combinations Differing Only in the Location of the 45° Sweptback Wing. NACA RM L7I01, 1947.

8. Donlan, Charles J., Myers, Boyd C., II, and Mattson, Axel T.: A Comparison of the Aerodynamic Characteristics at Transonic Speeds of Four Wing-Fuselage Configurations as Determined from Different Test Techniques. NACA RM L50H02, 1950.

TABLE I.- FUSELAGE COORDINATES

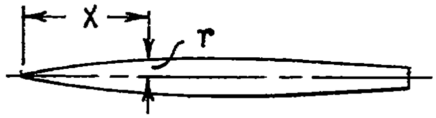

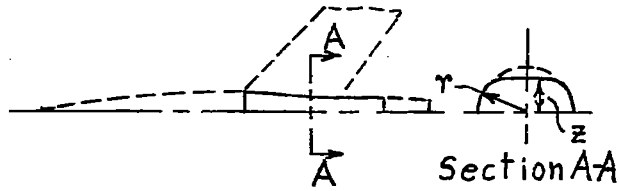

Standard fuselage coordinates	
x (in.)	r (in.)
0	0
.4	.185
.6	.238
1.0	.342
2.0	.578
4.0	.964
6.0	1.290
8.0	1.577
12.0	2.074
16.0	2.472
20.0	2.772
24.0	2.993
28.0	3.146
32.0	3.250
36.0	3.314
40.0	3.334
44.0	3.304
48.0	3.219
52.0	3.037
56.0	2.849
60.0	2.661
64.0	2.474
66.7	2.347

Indented fuselage coordinates		
x (in.)	z (in.)	r (in.)
40.0	3.334	3.334
41.0	3.299	-----
42.0	3.239	-----
43.0	3.173	-----
44.0	3.093	3.304
45.0	3.013	-----
46.0	2.940	-----
47.0	2.888	-----
48.0	2.860	3.219
49.0	2.858	-----
54.0	2.858	-----
55.0	2.853	-----
56.0	2.853	2.849
56.5	2.825	-----
60.0	2.661	2.661

NACA

TABLE II.- COORDINATES OF THE NACA 65A009 AIRFOIL

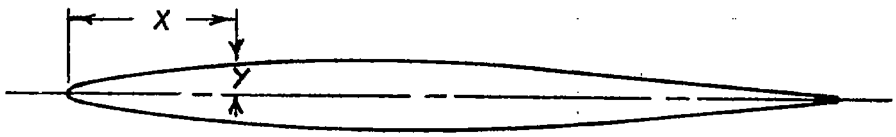

x/c (percent)	y/c (percent)
0	0
0.5	0.688
.75	.835
1.25	1.065
2.5	1.460
5.0	1.964
7.5	2.385
10.0	2.736
15.0	3.292
20.0	3.714
25.0	4.036
30.0	4.268
35.0	4.421
40.0	4.495
45.0	4.485
50.0	4.377
55.0	4.169
60.0	3.874
65.0	3.509
70.0	3.089
75.0	2.620
80.0	2.117
85.0	1.594
90.0	1.069
95.0	.544
100.0	.019
Leading-edge radius 0.575 percent C Trailing-edge radius 0.021 percent C	

NACA

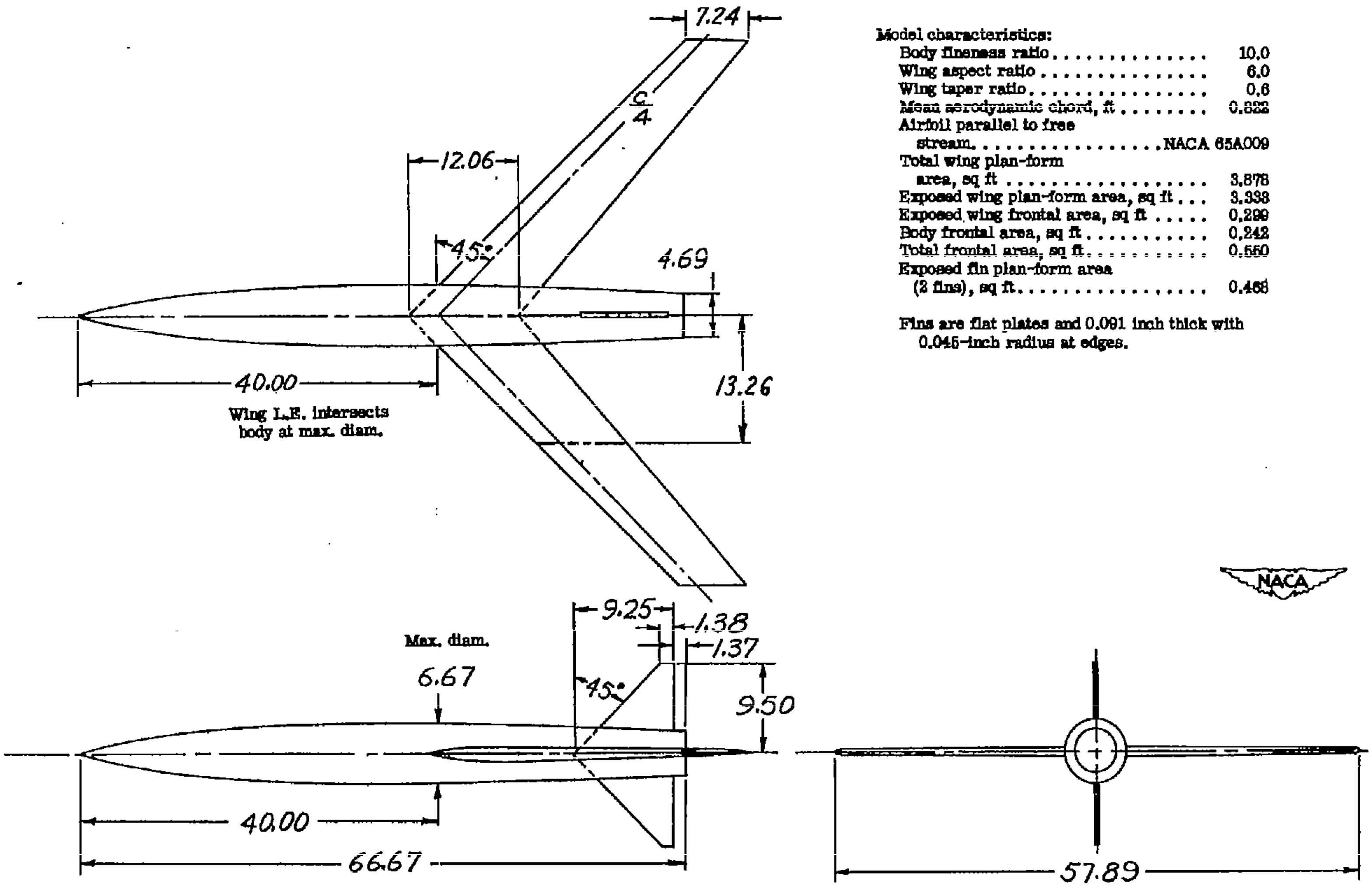

Model characteristics:

Body fineness ratio	10.0
Wing aspect ratio	6.0
Wing taper ratio	0.6
Mean aerodynamic chord, ft	0.822
Airfoil parallel to free stream	NACA 65A009
Total wing plan-form area, sq ft	3.878
Exposed wing plan-form area, sq ft	3.338
Exposed wing frontal area, sq ft	0.299
Body frontal area, sq ft	0.242
Total frontal area, sq ft	0.550
Exposed fin plan-form area (2 fins), sq ft	0.468

Fins are flat plates and 0.091 inch thick with 0.045-inch radius at edges.

Figure 1.- General arrangement and dimensions of test model. All dimensions are in inches.

NACA
L-61456

Figure 2.- Fuselage with four fins. Models A,B.

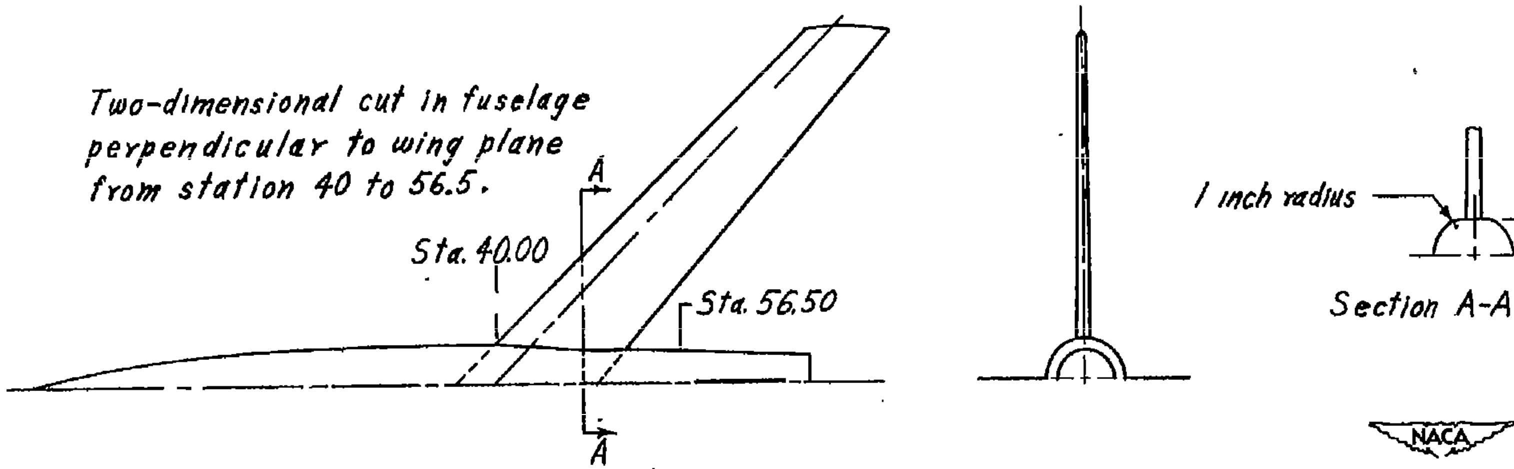

(a) Model D - modified fuselage.

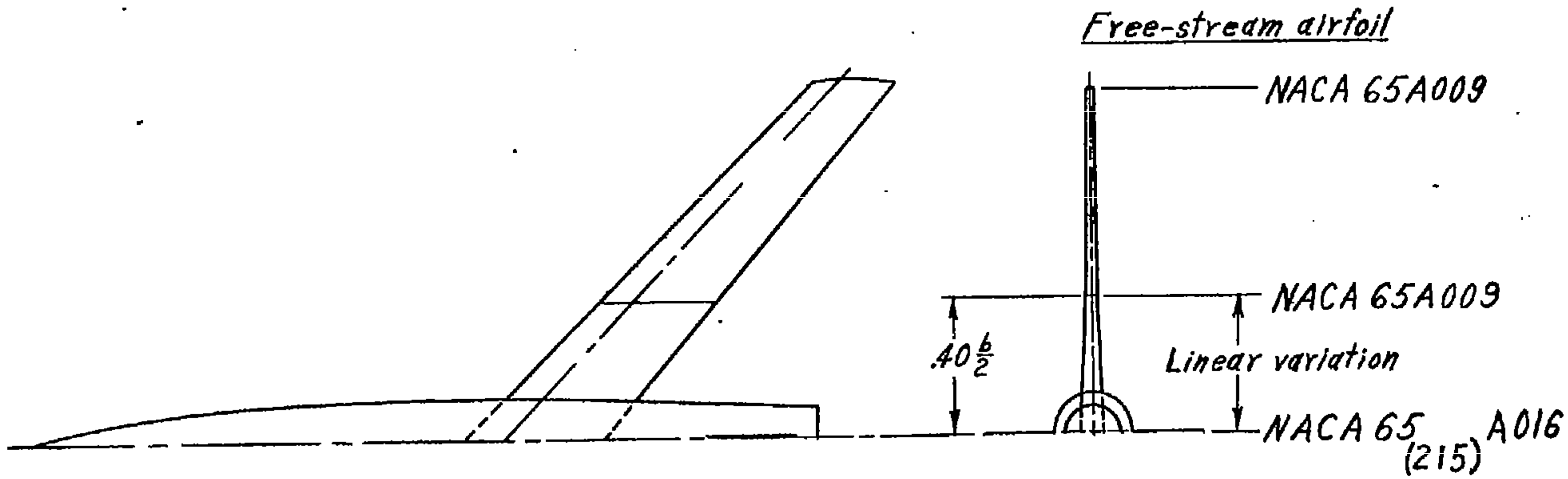

(b) Model E - modified wing.

Figure 3.- Arrangement of modified models.

(a) Plan view. L-68037.1

Figure 4.- Modified fuselage. Model D.

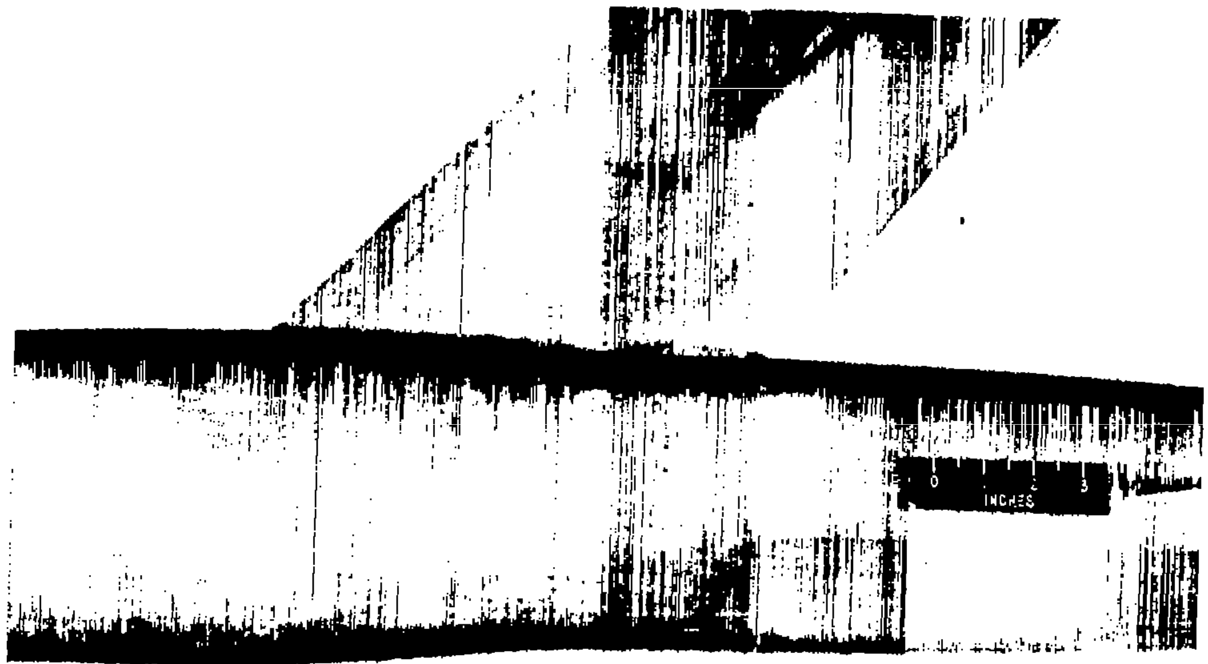

(b) Wing-fuselage intersection.

Figure 4.- Concluded.

L-68038.1

CONFIDENTIAL

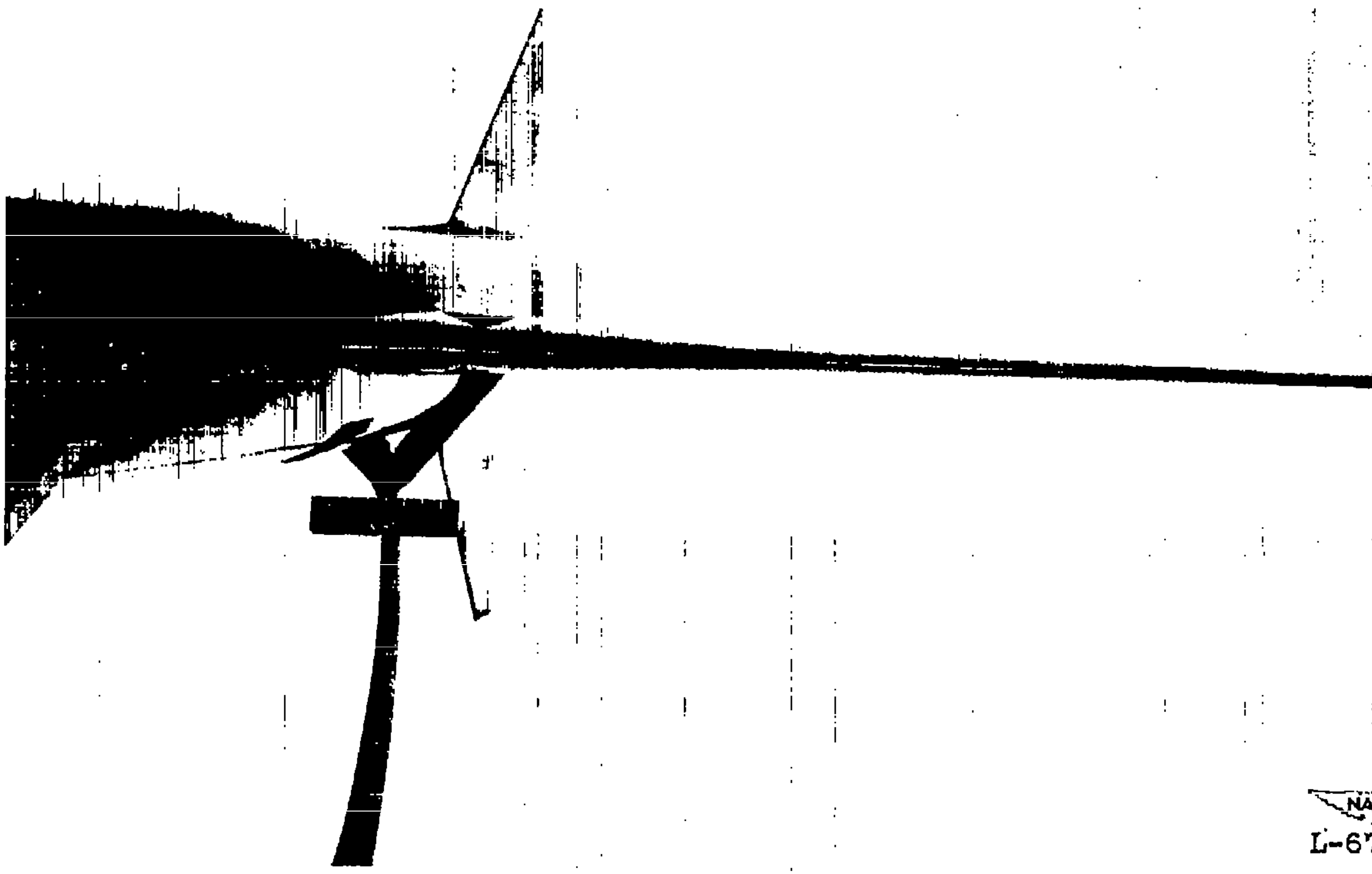

L-67472

Figure 5.- Front three-quarter view of thickened wing root. Model E.

CONFIDENTIAL

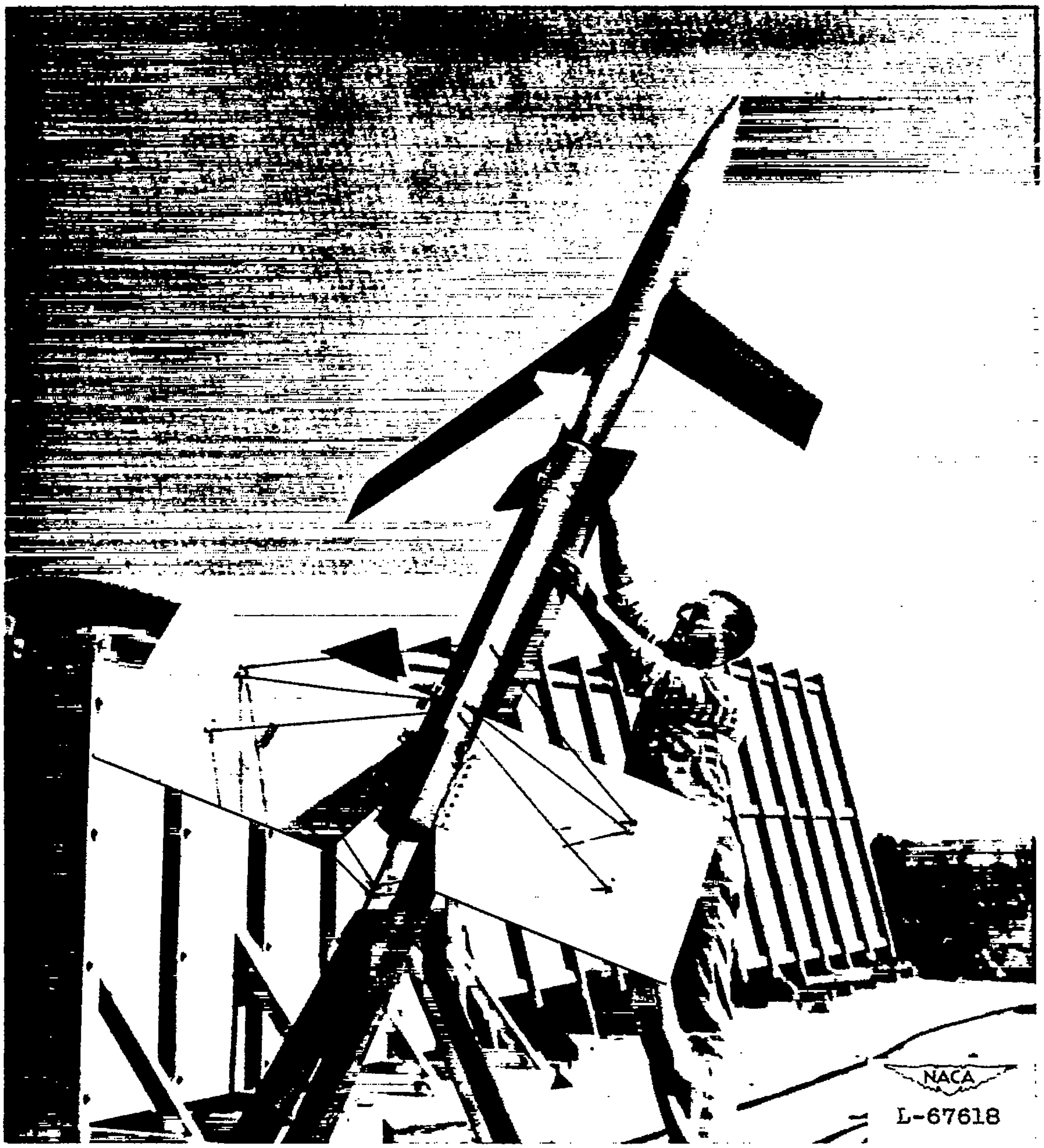

Figure 6.- Model E and booster on rail launcher.

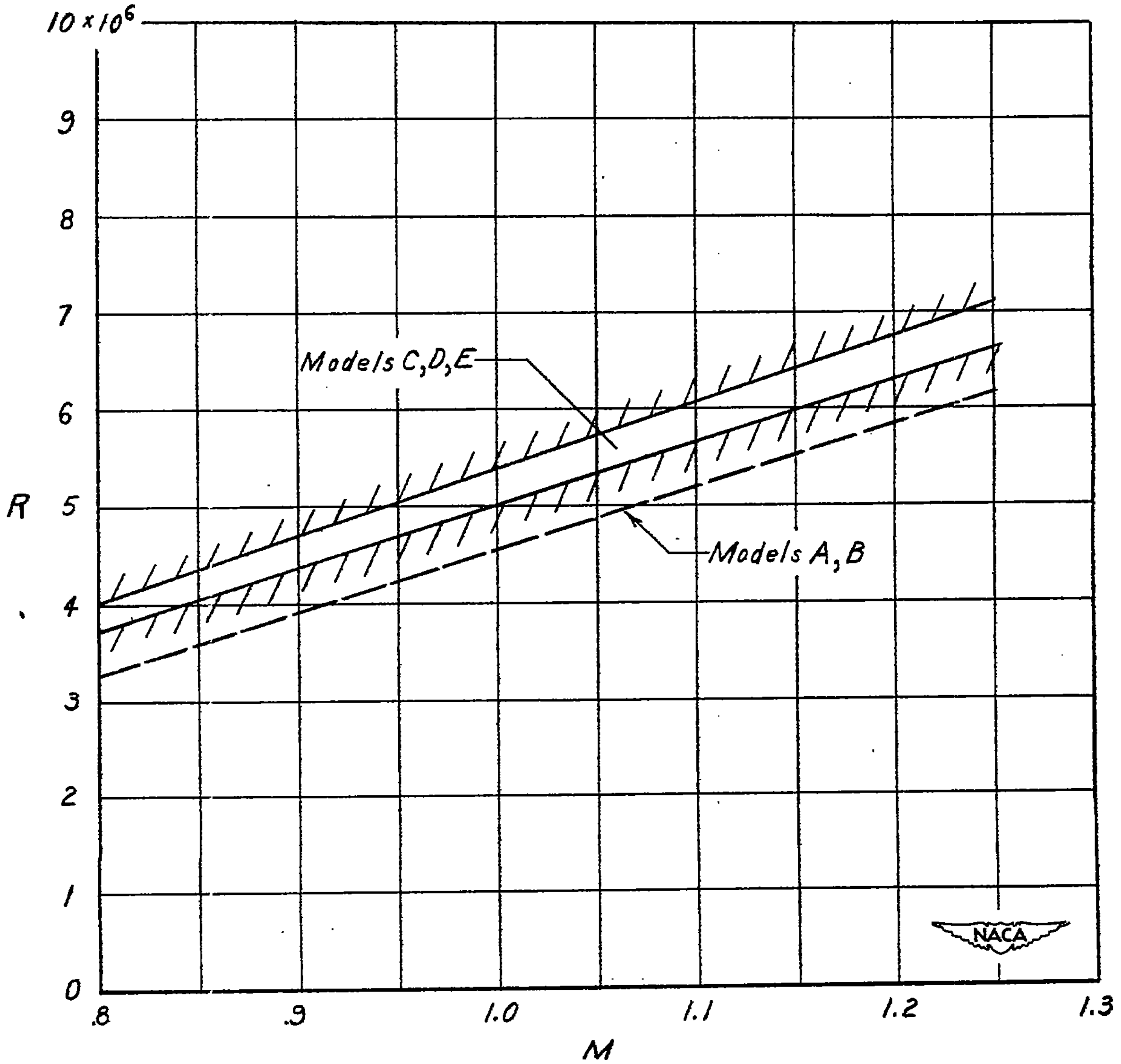

Figure 7.- Variation of Reynolds number range with Mach number for models tested. (Based on wing mean aerodynamic chord.)

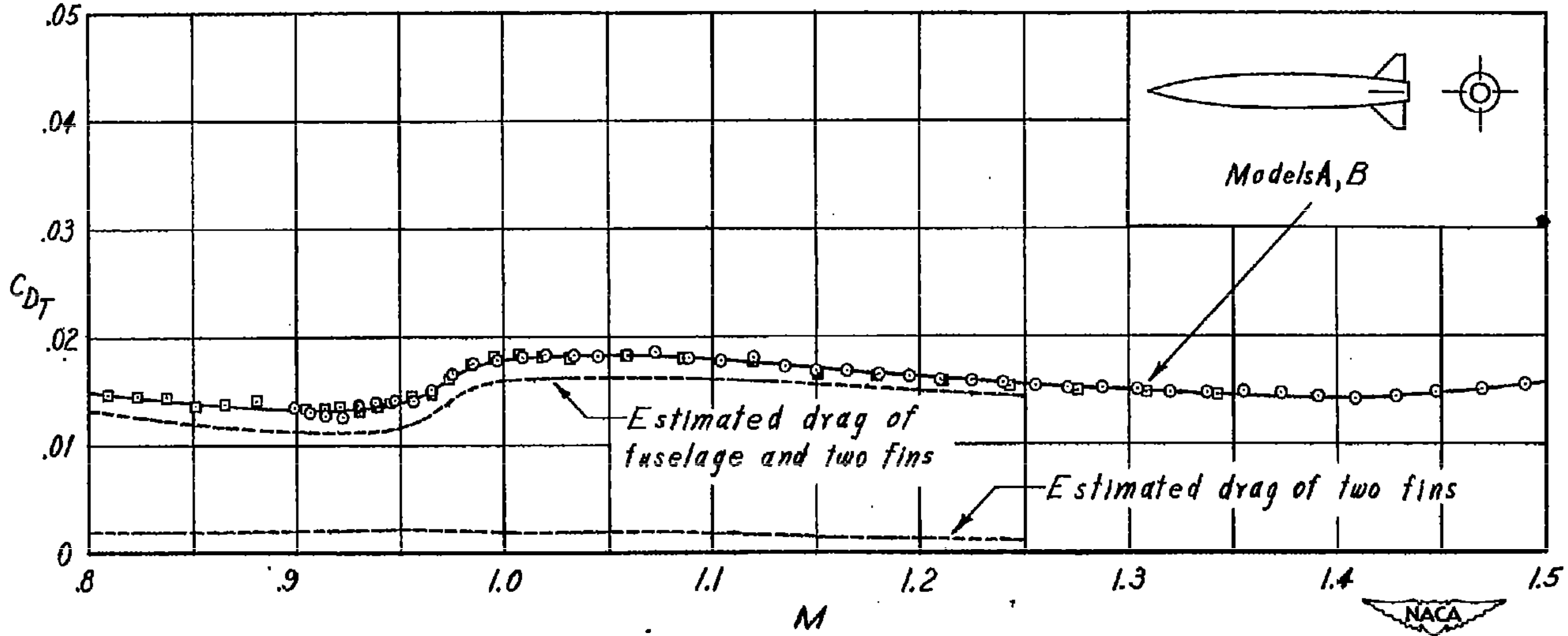

Figure 8.- Variations of fuselage drag coefficient with Mach number for configurations with two and four fins. (Based on wing plan-form area.)

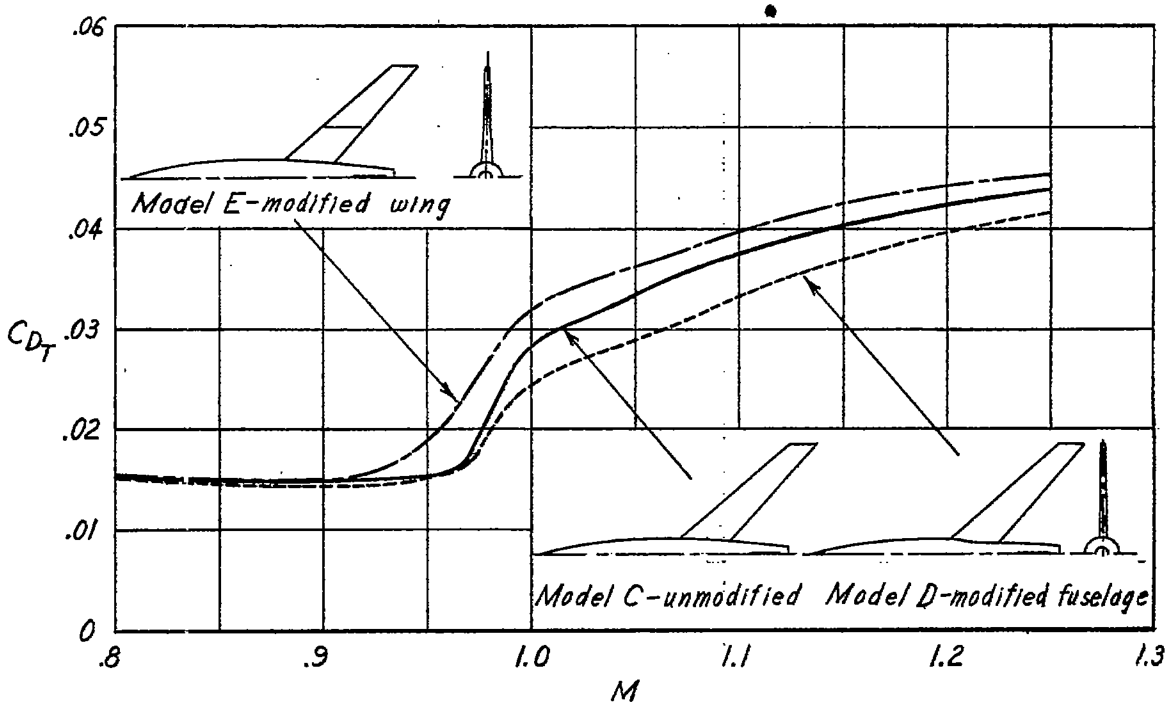

(a) Total drag coefficient.

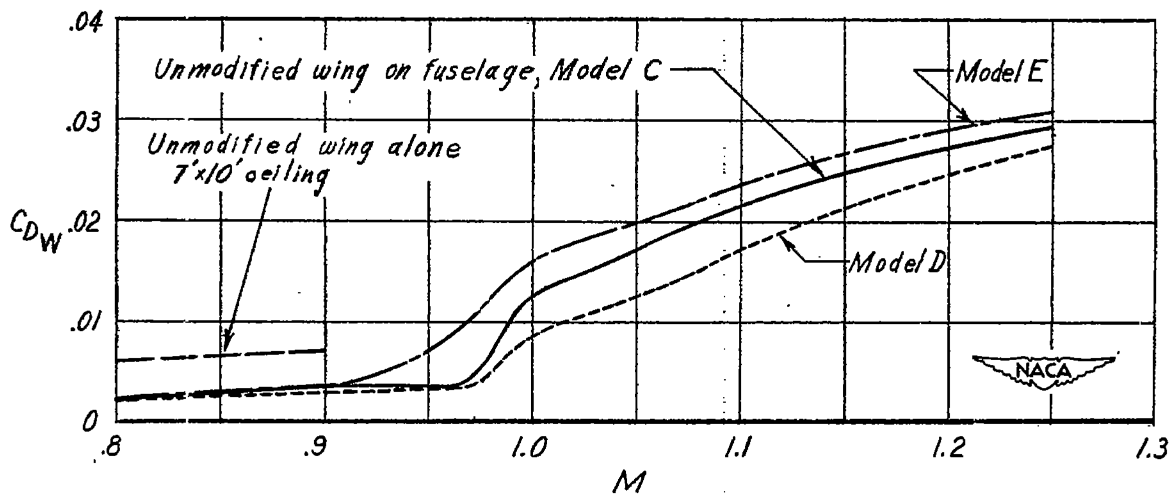

(b) Wing-plus-interference drag coefficient.

Figure 9.- Variations of total drag and wing-plus-interference drag coefficients with Mach number for the unmodified, modified fuselage, and modified wing models. (Based on wing plan-form area.)